Journal of
Chemical Engineering & Process Technology

Shrestha, J Chem Eng Process Technol 2016, 7:3
DOI: 10.4172/2157-7048.1000295

Research Article Open Access

Chemical, Structural and Elemental Characterization of Biosorbents Using FE-SEM, SEM-EDX, XRD/XRPD and ATR-FTIR Techniques

Sohan Shrestha*

Nepal Academy of Science and Technology, Lalitpur, Bagmati Zone, Nepal

Abstract

The chemical, structural, and elemental composition of any adsorbents plays undoubtedly crucial role and has paramount significance in adsorption process. The present study of chemical, structural, and elemental characterization of powdered *Pinus densiflora* pine cones, lignite and coconut shell-based activated carbon fiber (ACF), and powdered oyster shell prior employed for anionic surfactant sodium dodecyl sulfate (SDS) adsorption was undertaken using field emission scanning electron microscope (FE-SEM), scanning electron microscope coupled with energy dispersive x-ray (SEM-EDX), X-ray diffraction/X-ray powder diffraction (XRD/XRPD), and multiple internal reflectance (MIR) or attenuated transform reflectance – fourier transform infrared spectroscopy (ATR-FTIR) techniques. The FE-SEM imaging observed at three different magnifications depicted the change in surface texture of aforementioned biosorbents before and after SDS adsorption. SEM-EDX analysis indicated alteration in the concentration and distribution of different compositional elements. The XRD analysis suggested the amorphous character in lignite and coconut shell-based ACF and powdered *Pinus densiflora* cones, whilst indicating the sample of powdered oyster shell to be crystalline in nature and entirely composed of $CaCO_3$ with the very trivial amount of impurities. Further, infra-red (IR) spectroscopy demonstrated variation in IR spectra of the samples prior to and after surfactant adsorption and also further suggested occurrence of complexing or (complexation) process between ionizable functional groups and DS^- or Na^+ ions of SDS. In addition, iodine number of the lignite and coconut shell-based ACF, powdered *Pinus densiflora* cones, and powdered oyster shell were found to be 285.86 mg/g, 25.01 mg/g, and 28.48 mg/g, respectively.

Keywords: Biosorbents; FE-SEM; SEM-EDX; FTIR; XRD

Introduction

Given the increased emphasis on the use of lignite and coconut shell-based activated carbon fiber (ACF), powdered oyster shell, and acidified powdered *Pinus densiflora* (Japanese red pine) pine cones as the prominent biosorbents for anionic surfactant sodium dodecyl sulfate (SDS) adsorption, there have been surprisingly few studies undertaken to characterize the chemical, structural, and elemental composition of aforementioned samples. The main aim of this study, therefore was to investigate the chemistry, structure, and mineralogy of lignite and coconut shell-based activated carbon fiber (ACF), powdered oyster shell, and powdered *Pinus densiflora* pine cones samples using multiple characterization techniques including x-ray diffraction (XRD)/x-ray powder diffraction (XRPD) analysis, field emission scanning electron microscopy (FE-SEM), multiple internal reflectance (MIR) or attenuated transform reflectance – fourier transform infrared spectroscopy (ATR-FTIR), scanning electron microscopy coupled with energy dispersive x-ray (SEM-EDX). In addition, the samples were treated to determine the iodine number or iodine index for the characterization of the three samples. Results will provide an evaluation of the key differences in structure, chemical, and elemental composition of aforementioned samples (adsorbents) prior to and after anionic surfactant adsorption.

Materials and Methods

Materials

The lignite and coconut shell-based activated carbon fiber (ACF) used in the present study was procured from Korea ACF Co. Ltd. Similarly, the naturally occurring cones of *Pinus densiflora* were collected from the premises of Kumoh National Institute of Technology (KIT), Gumi. Meanwhile, the oyster shells were fetched from the beach of Pohang, South Korea.

Biomodification of the samples

The lignite and coconut shell-based activated carbon fiber was used in the experimentation without further processing as procured, while the oyster shells were pre-treated before use by washing thoroughly with the distilled water and dried at the temperature of 110 ± 2°C for 24 h in an oven. Further, the raw biosorbent was crushed and ground into the powder form using grinder mixture. The biosorbent was again washed thoroughly with the distilled water and dried naturally. The resulted shell particles were stored in sterile, sealed plastic bottle and used in the experimentation. On the other hand, the cones was also pre-treated prior to its use by washing thoroughly with the distilled water and then dipped into the 2.0% concentrated HCl solution for 12 h. The acidified pine cones were then dried at the temperature of 110 ± 2°C for 24 h in an oven. Further, the cones were crushed and ground into the powder form. The powdered pine cones were kept in sealed plastic bottle and employed for all the adsorption experiments.

Methods

Iodine number (or iodine index) determination for characterization of adsorbents: In determining the iodine number of lignite and coconut shell-based acivated carbon fiber, 0.1 g of adsorbent was placed with 25 mL of iodine solution in a 250 mL conical flask and was shaken for 1 min. After that the solution was filtered and 10 mL of

***Corresponding author:** Sohan Shrestha, Nepal Academy of Science and Technology, Lalitpur, Bagmati Zone, Nepal, E-mail: scientist.nepalensis@gmail.com

Received January 25, 2016; **Accepted** May 19, 2016; **Published** May 26, 2016

Citation: Shrestha S (2016) Chemical, Structural and Elemental Characterization of Biosorbents Using FE-SEM, SEM-EDX, XRD/XRPD and ATR-FTIR Techniques. J Chem Eng Process Technol 7: 295. doi:10.4172/2157-7048.1000295

the filtrate was taken in a conical flask. The solution was titrated with 0.01 N sodium thiosulfate solution until it become clear. The iodine number of the activated carbon was determined by using Eq. (1) which represents the number of milligrams of iodine adsorbed by one gram of activated carbon [1]:

$$Iodinenumber = \frac{V \times (T_i - T_f) \times C_i \times M_i}{T_i \times g} \quad (1)$$

where, V is the volume of iodine solution (25 mL); T_i is the volume of sodium thiosulfate solution used for the titration of 10 mL iodine solution; T_f is the volume of sodium thiosulfate solution used for the titration of 10 mL filtrate; g represents the weight of adsorbent (0.1 g); M_i is the molar weight of iodine (126.9044 g/mol); and C_i is the concentration of iodine solution (0.01 N).

Similarly, 1.0 g of adsorbent was placed with 25 mL of iodine solution in a 250 mL conical flask and was shaken for 1 min for determining the iodine number in the present study, whilst the other procedures are same as aforementioned in case of ACF.

Infra-red (IR) spectroscopy (ATR-FTIR): In order to detect the functionality present in lignite and coconut shell-based ACF, powdered oyster shell, and powdered *Pinus densiflora* pine cones prior to and after anionic surfactant, i.e., sodium dodecyl sulfate (SDS) adsorption, FTIR spectroscopy studies using attenuated total reflectance (ATR) or multiple internal reflectance (MIR) apparatus were carried out by VERTEX 80v, Fourier Transform Infrared Spectrometer, Bruker Optics Korea Co., Ltd (Germany). Adsorption in the infrared (IR) region takes place due to the rotational and vibrational movement of the molecular groups and chemical bond of a molecule [2].

Scanning electron microscopy (FE-SEM): The surface morphology of lignite and coconut shell-based ACF, powdered oyster shell, and powdered *Pinus densiflora* pine cones before and after SDS adsorption were observed using Field Emission Scanning Electron Microscope (FE-SEM). The samples for FE-SEM observation were first cut into small pieces in accordance with the requirement, before placed on the sample – stubs. Prior to scanning, the samples were attached to the sample holder and coated with gold using sputter – cutting (SEM Coating System Machine). Samples were scanned using JEOL JSM – 6701F FE-SEM operating at 15 kV.

Scanning electron microscope and energy dispersive X-ray microanalysis (SEM-EDX): All the samples were observed from SEM, with elemental compositions being analyzed by EDX. After air-dried, the samples were passed through a 0.65 micrometer of filter paper. Then, samples were mounted on stubs with conductive carbon tape and coated with carbon. All samples were analyzed for their micro-structure and elemental compositions under JEOL JSM – 6701F FE-SEM operating at 15 kV.

X-ray diffraction (XRD): The X-ray powder diffraction spectra (XRD data) were taken by employing using 10 mm × 10 mm beam size, graphite-monochromated Cu/Kα radiation (λ=1.5406 Å) at 40 kV and 100 mA. The 2θ ranges were from 10° to 90° in the step of 2.0°. The detection of the powder X-ray diffraction pattern was performed by using SWXD Diffractometer, Rigaku Corporation (Japan) operating at 18 kW, which collects the two-dimensional diffraction patterns of the sample. Data were processed using the D/MAX – 2000/PC version 3.0.0.0 ~ software.

Results and Discussion

Determination of iodine number

Iodine number is one of the most essential parameters widely used to characterize the adsorbents [3]. It was found that iodine number of the lignite and coconut shell-based activated carbon fiber used in the present study as an adsorbent was found to be 285.86 mg/g. It was found that iodine numbers of powdered *Pinus densiflora* cones and powdered oyster shell were 25.01 mg/g and 28.48 mg/g, respectively. Thus, lignite and coconut shell-based ACF could be considered far better adsorbent in comparison to powdered *Pinus densiflora* cones and powdered oyster shell on the basis of iodine index as iodine is the most common standard adsorbate.

ATR-FTIR studies

IR spectra of powdered *Pinus densiflora* cones before and after SDS adsorption are shown in Figure 1. Similarly, the main frequencies of vibrations and their corresponding functional groups that interacted with the SDS during the adsorption process are presented in Table 1.

It is apparent that there were some changes in the absorption peak frequencies from infrared (IR) spectra prior to and after SDS adsorption. It was observed that absorption peak frequencies, i.e., 1631.04 cm^{-1}, 1567.09 cm^{-1}, 1770.14 cm^{-1}, and 3482.55 cm^{-1} were devoid in SDS loaded IR spectrum, corresponding to the carboxamide (C=O stretching vibrations), carboxylate, acid (aryl) halide, and aromatic 1° (primary) amine (N-H stretching) functional groups, respectively. Meanwhile, absorption band frequencies 2881.82 cm^{-1} and 2946.66 cm^{-1} corresponding to the C-H stretching in alkanes were not observed in SDS free spectrum (Figure 2).

On the other hand, the SDS loaded spectrum demonstrated minor changes in absorption peak frequencies corresponding to various other functional groups with the exception of major shift in the positions of O-H stretching in alcohol, C=O stretching in aldehydes or ketones, C-N stretching vibration in 2° (secondary) amine, and 1,4-disubstitution (para) in C-H bonding, i.e., from 3842.55 to 3484.73 cm^{-1}, 1706.99 to 1707.49 cm^{-1}, 1139.83 to 1140.06 cm^{-1}, and 848.38 to 843.31 cm^{-1}, respectively (Table 1).

It is well familiar that the electrostatic interactions are not strong enough to shift the absorption band of the functional groups present on the adsorbent surface [4]. Consequently, these shifts suggested complexing or (complexation) process took place between ionizable functional groups and DS^{-}or Na^{+} ions of SDS. In conclusion, the results obtained were suffice enough to draw a bottom line conforming the occurrence of chemical complexation between DS^{-}or Na^{+} ions of SDS and various functional groups present on the surface of powdered cones.

The ATR-FTIR spectroscopy studies were undertaken to elaborate the adsorption mechanism governing the SDS adsorption on lignite and coconut shell-based activated carbon fiber. It was observed that absorption band frequency 2881.72 cm^{-1} corresponding to C-H stretching of methyne and 737.34 cm^{-1} corresponding to C-Cl stretching of aliphatic chloro-compounds were absent in SDS loaded spectrum as depicted in Ref. [5] (Figure 2).

On the other hand, the SDS loaded IR spectrum demonstrated minor changes in absorption peak frequencies corresponding to various other functional groups with the exception of noticeable major changes in the positions of O-H stretching (alcohol), C-N stretching (2° amine), N-H stretching (aromatic 1° amines), C=O stretching (carboxylic acid

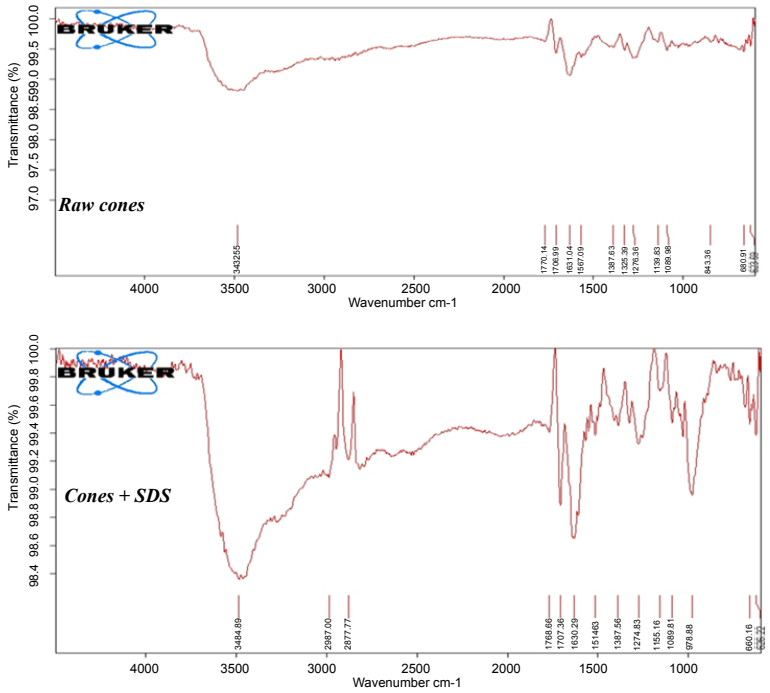

Figure 1: ATR-FTIR spectra absorption band/peak frequencies and corresponding possible functional groups of powdered pine cone before and after SDS adsorption.

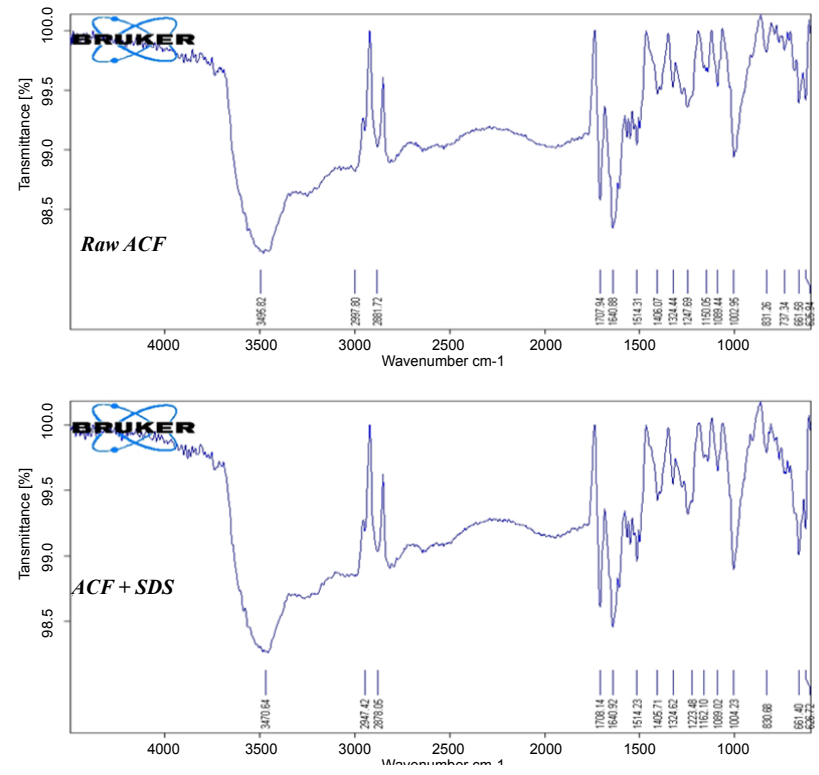

Figure 2: ATR-FTIR spectra absorption band/peak frequencies and corresponding possible functional groups of ACF before and after SDS adsorption.

Wave numbers (cm^{-1})		Corresponding functional groups
Before SDS adsorption	After SDS adsorption	
3482.55	3484.73	Alcohol, hydroxy group (O-H stretching) (broad band)
-	2881.82, 2946.66	Alkane (C-H stretching)
3482.55, 1631.04, 1567.09	3484.73, 1628.41	1° amines (N-H stretching)
1706.99	1707.49	Aldehydes or ketones (R-COR, C=O stretching)
1706.99, 1770.14	1707.49, 1768.63	Carboxylic acid (R-COOH) (C=O stretching)
1631.04	-	Amide (Carboxamide) ($R\text{-}CONR_2$) (R = H or C) (C=O stretching)
1631.04	1628.41	Alkene (C=C stretching)
1089.98, 1139.83, 1276.83	1031.20, 1089.38, 1140.06, 1277.82	Alcohol or ether (C-OH)
848.38	843.31	1,4-disubstitution (para) in C-H bonds (aromatic ring bending)
660.91, 623.59	623.42	Aliphatic organohalogen compounds (C-Br stretching)
1089.98, 1139.83	1089.38, 1140.06	Cyanate (-OCN and C-OCN stretching)
1089.98	1031.20, 1089.38	Organic siloxane or silicone (Si-O-Si)
1567.09	-	Carboxylate (carboxylic acid salt)
1770.14	-	Acid (acyl) halide
3482.55	-	Aromatic 1° amine (N-H stretching)
1139.83	1140.06	Secondary amine (C-N stretch)

Table 1: IR absorption bands and corresponding possible functional groups of powdered *Pinus densiflora* (Japanese red pine) cones prior to and after SDS adsorption.

or ketones), and P-O-C stretching (aliphatic phosphates), i.e., 3495.82 to 3470.64 cm^{-1}, 1150.05 to 1162.1 cm^{-1}, 3495.82 to 3470.64 cm^{-1}, 1707.94 to 1708.14 cm^{-1}, and 1002.95 to 1004.23 cm^{-1}, respectively as shown in Table 2 (Coates). Consequently, these shifts suggested that the complexing process took place between the ionizable functional groups present on the adsorbent surface and DS^{-}or Na^{+} ions [4]. However, minor changes in absorption peak frequencies corresponding to various other functional groups after SDS adsorption corroborated that there was no significant and strong coordination between DS^{-}or Na^{+} ions and functional groups at those sites.

It is apparent that there were some changes in absorption peak frequencies or wave numbers from IR spectra in powdered oyster shell prior to and after SDS adsorption as shown in Figure 3 [5,6]. As shown in Table 3 [5], the SDS loaded spectrum demonstrated minor changes in absorption peak frequencies corresponding to various other functional groups with the exception of major shift or changes in the positions of C-H stretching in methyne, C-N stretching in 2° or 3° amine, C=O stretching in carboxyl (carboxylic acid) or carbonyl (ketones) groups, and C=O stretching vibrations in acyl halide (or haloformyl group), i.e., 2883.08 to 2878.84 cm^{-1}, 1150.78 to 1139.74 cm^{-1}, 1707.24 to 1706.83 cm^{-1}, and 1798.11 to 1797.73 cm^{-1}, respectively [5-8]. It is well known that the electrostatic interactions are not strong enough to shift the absorption band frequencies or wavenumbers of the functional groups present on the adsorbent surface [4]. Consequently, these shifts suggested that there was complexing process taking place between the ionizable functional groups and DS^{-}or Na^{+} ions of SDS. However, minor changes in absorption peak frequencies corresponding to various other functional groups after SDS adsorption corroborated that there was weak coordination between the DS^{-}or Na^{+} ions and functional groups at those sites [4].

Field Emission Scanning Electron Microscope (FE-SEM) studies

The surface textural characterization of powdered pine cones, lignite and coconut shell-based ACF, and powdered oyster shell prior to and after SDS adsorption were carried out using Field Emission Scanning Electron Microscope (FE-SEM) at various magnifications. Further, the surface textures of powdered pine cones (Figure 4), lignite and coconut shell-based ACF (Figure 5), and powdered oyster shell (Figure 6) prior to SDS adsorption were observed to be smooth and regular with less undulations, i.e., less degree of roughness and waviness, while the surface morphology of powdered pine cones (Figure 7), lignite and coconut shell-based ACF (Figure 8), and powdered oyster shell (Figure 9) were observed to be rough with more undulations, i.e., high degree of roughness and waviness, after the biosorbents were subjected to adsorption process at various magnifications ranging from X5000, X10000, and X30000.

Microanalysis of structural and elemental composition of biosorbents using SEM-EDX technique

Scanning electron microscope and energy dispersive X-ray microanalysis (SEM-EDX) determined the micro-structure and elemental composition of *Pinus densiflora* cones, lignite and coconut shell-based activated carbon fiber, and powdered oyster shell as depicted in aforementioned (Figures 10-12).

EDX detected the emission of elements of carbon (C), oxygen (O), and chlorine (Cl). The percentage (wt%) of all elements before SDS adsorption was investigated as following order: C (62.30%) > O (37.07%) > Cl (0.63%) (Figure 10). Similarly, the percentage (wt%) of all elements present in *Pinus densiflora* cone after adsorption was investigated as following order: C (62.24%) > O (37.65%) > Cl (0.10%) (Figure 10).

As shown in Figure 11, EDX detected the presence of elements of carbon (C), oxygen (O), sodium (Na), and phosphorus (P). The percentage (wt%) of all elements present in ACF was investigated as following order (before adsorption) (Figure 11): C (82.37%) > O (15.79%) > P (1.66%) > Na (0.18%). Similarly, the percentage (wt%) of all elements present in ACF was investigated as following order (after adsorption): C (77.12%) > O (21.39%) > P (1.42%) > Na (0.08%) (Figure 11).

As shown in Figure 12, EDX detected the presence of elements of carbon (C), oxygen (O), magnesium (Mg), sulfur (S), calcium (Ca), and tin (Sn). The percentage (wt%) of all elements present in powdered oyster shell was investigated as following order (before adsorption) (Figure 12): O (55.69%) > Ca (33.10%) > C (9.82%) > Sn (0.84%) > S

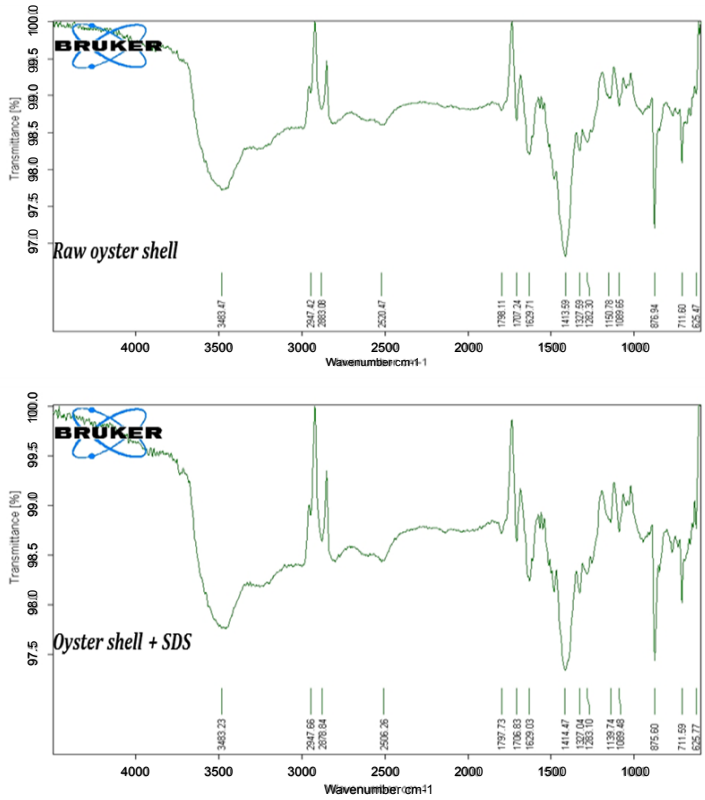

Figure 3: ATR-FTIR spectra absorption band/peak frequencies and corresponding possible functional groups of powdered oyster shell before and after SDS adsorption.

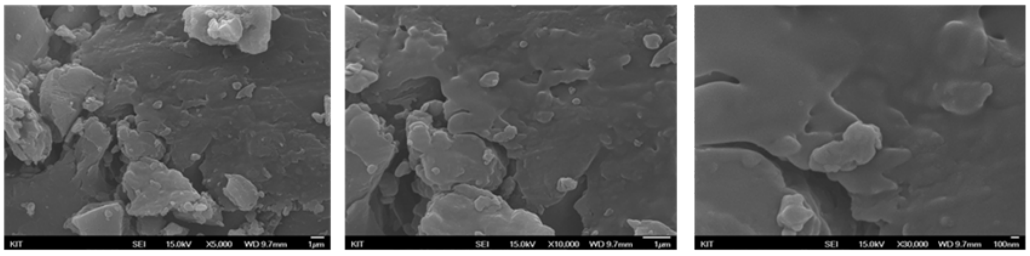

(a) (b) (c)

Figure 4: FE-SEM images of *Pinus densiflora* cone before SDS adsorption at various magnifications, i.e., (a) X5000; (b) X10,000; (c) X30,000.

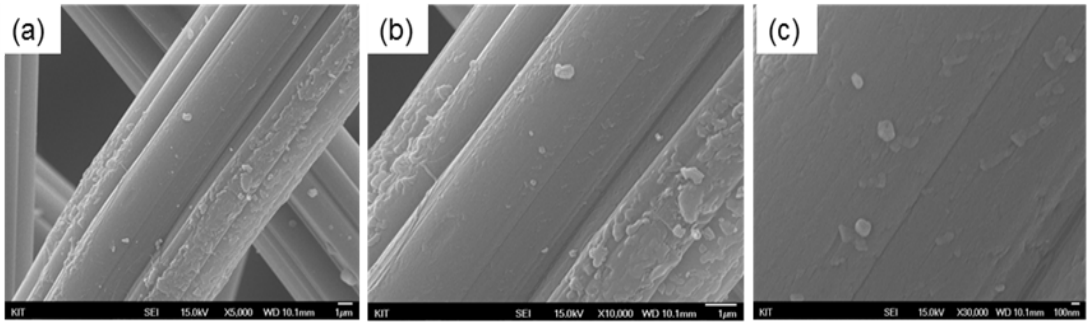

Figure 5: FE-SEM images of lignite and coconut shell-based activated carbon fiber before SDS adsorption at various magnifications, i.e., (a) X5000; (b) X10,000; (c) X30,000.

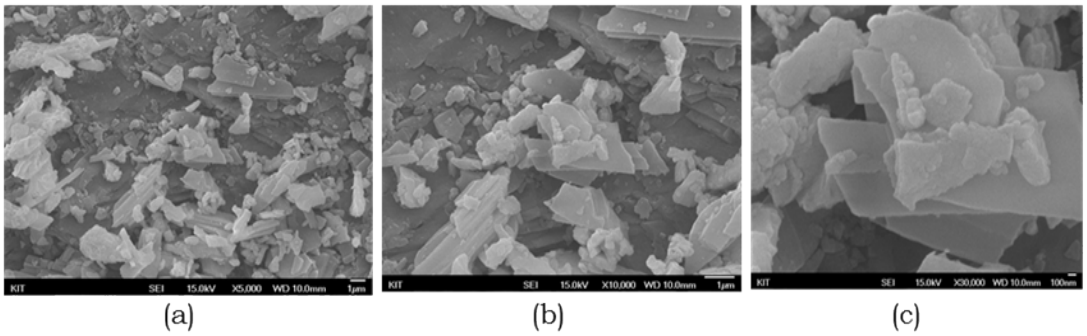

Figure 6: FE-SEM images of Oyster shell before SDS adsorption at various magnifications, i.e., (a) X5000; (b) X10,000; (c) X30,000.

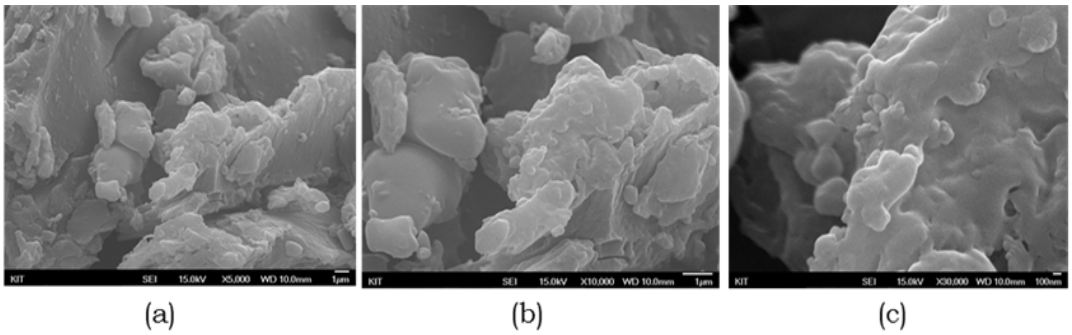

Figure 7: FE-SEM images of *Pinus densiflora* cone after SDS adsorption at various magnifications, i.e., (a) X5000; (b) X10,000; (c) X30,000.

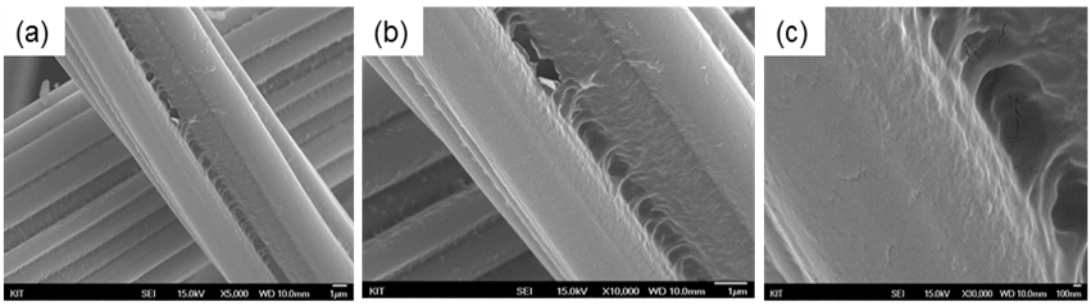

Figure 8: FE-SEM images of lignite and coconut shell-based activated carbon fiber after SDS adsorption at various magnifications, i.e., (a) X5000; (b) X10,000; (c) X30,000.

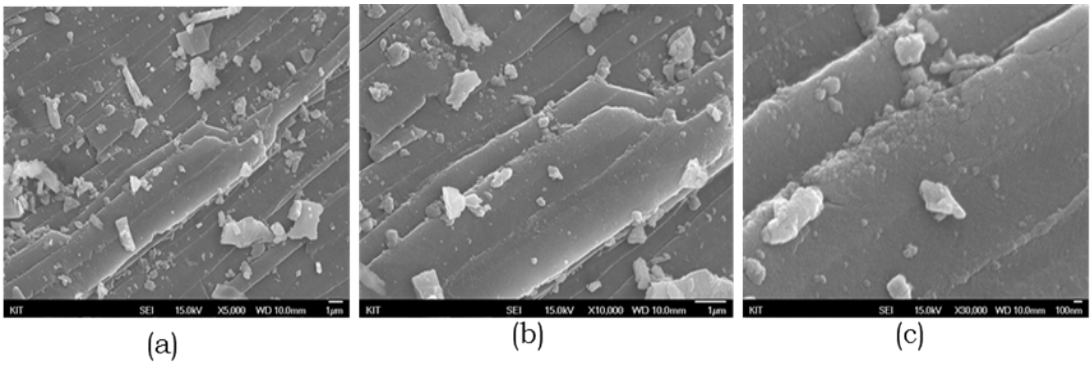

Figure 9: FE-SEM images of Oyster shell after SDS adsorption at various magnifications, i.e., (a) X5000; (b) X10,000; (c) X30,000.

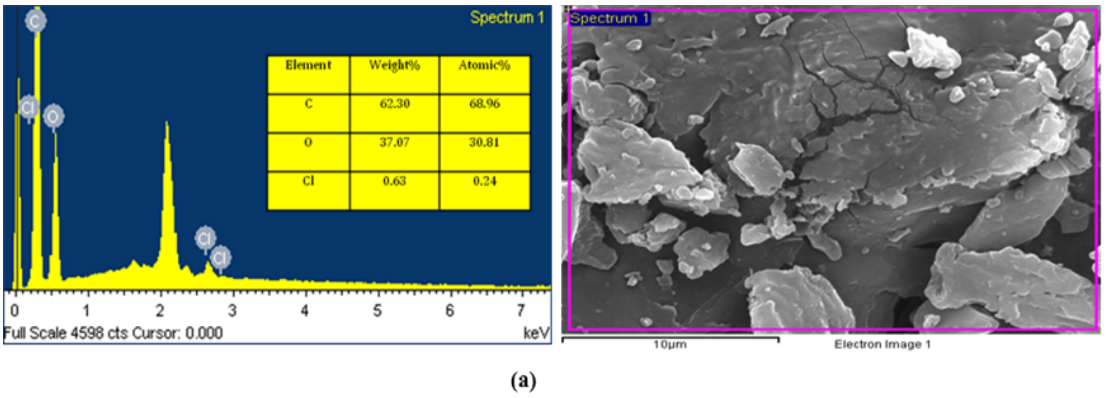

(a)

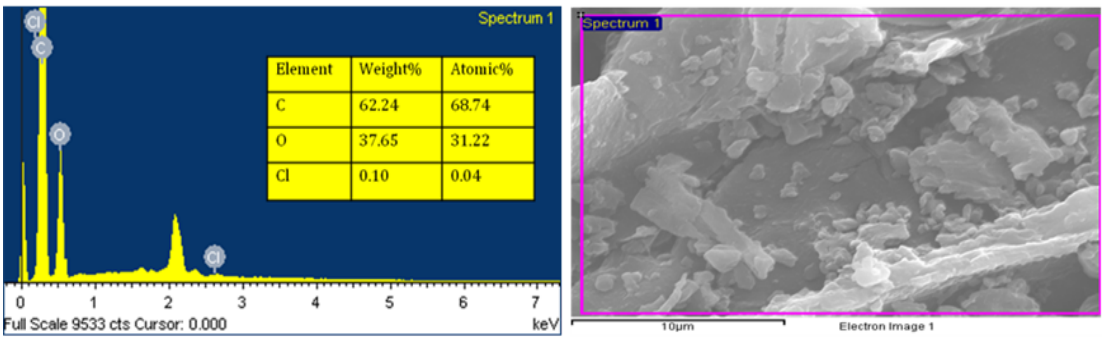

(b)

Figure 10: SEM-EDX image of *Pinus densiflora* cones powder before SDS adsorption (a); and after SDS adsorption (b) at the magnification of X5000.

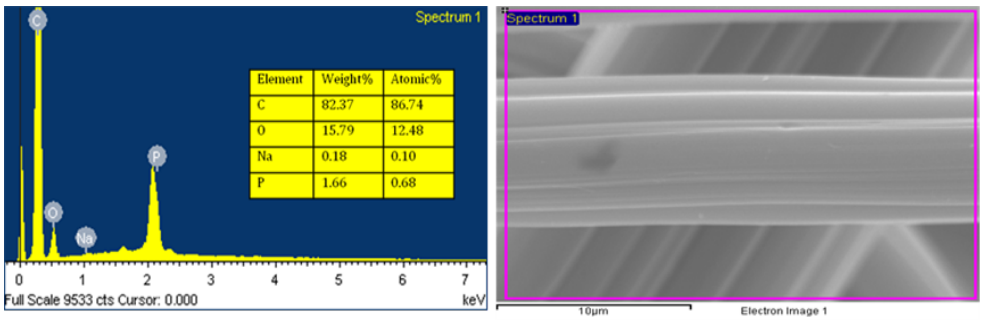

(a)

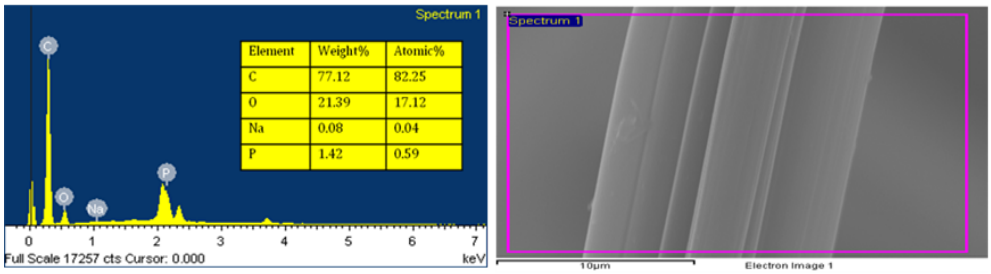

(b)

Figure 11: SEM-EDX image of lignite and coconut shell-based ACF before SDS adsorption (a); and after SDS adsorption (b) at the magnification of X5000.

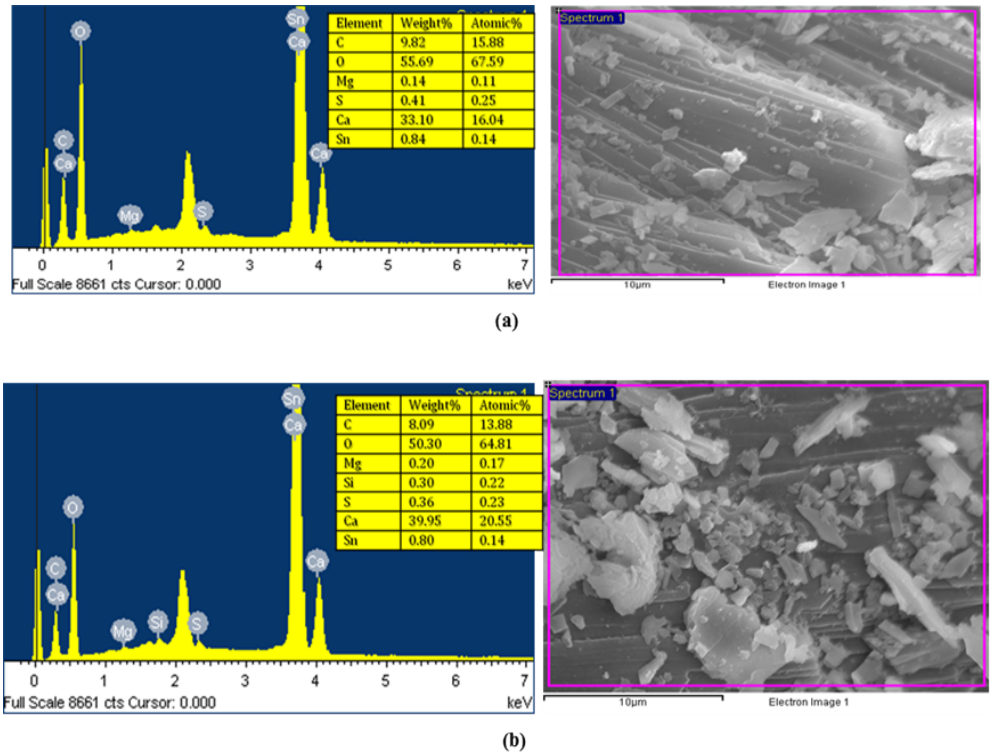

Figure 12: SEM-EDX image of powdered oyster shell before SDS adsorption (a); and after SDS adsorption (b) at the magnification of X5000.

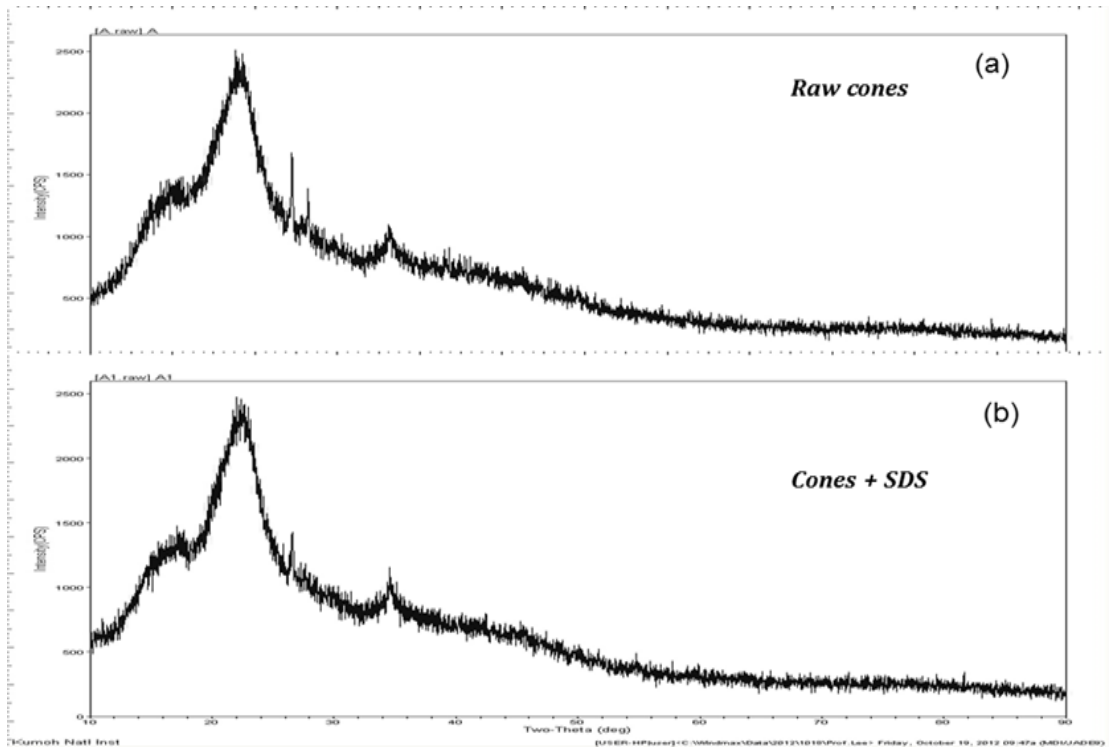

Figure 13: XRD pattern of powdered *Pinus densiflora* cone before SDS adsorption (a) and after SDS adsorption (b).

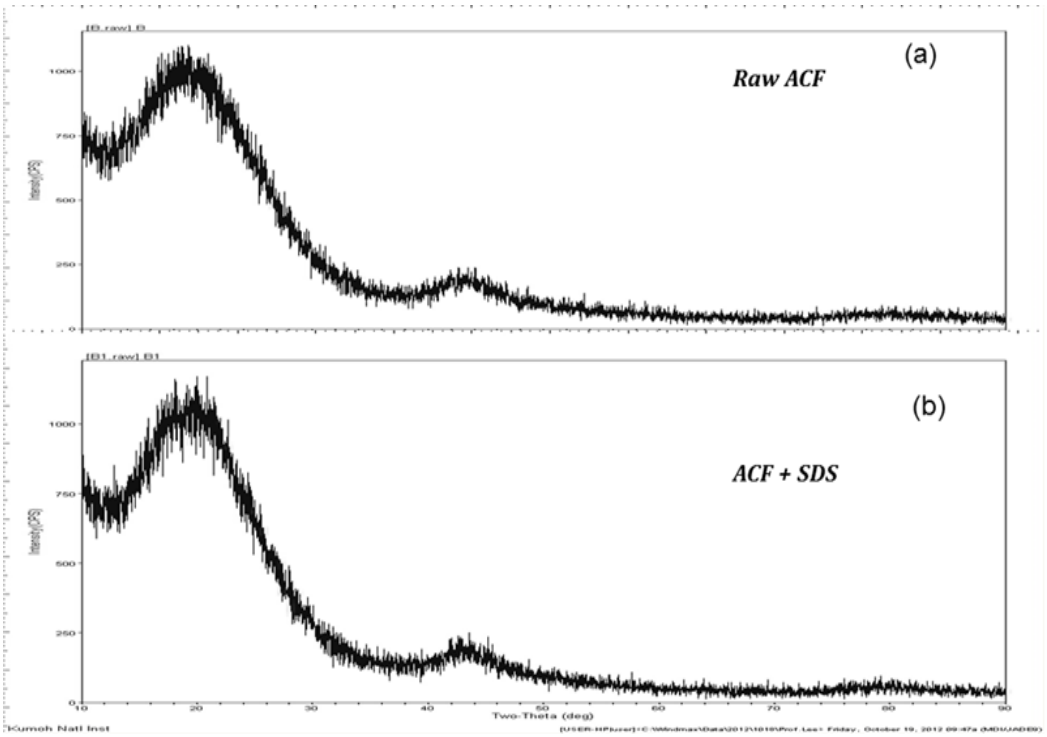

Figure 14: XRD pattern of lignite and coconut shell-based activated carbon fiber before SDS adsorption (a) and after SDS adsorption (b).

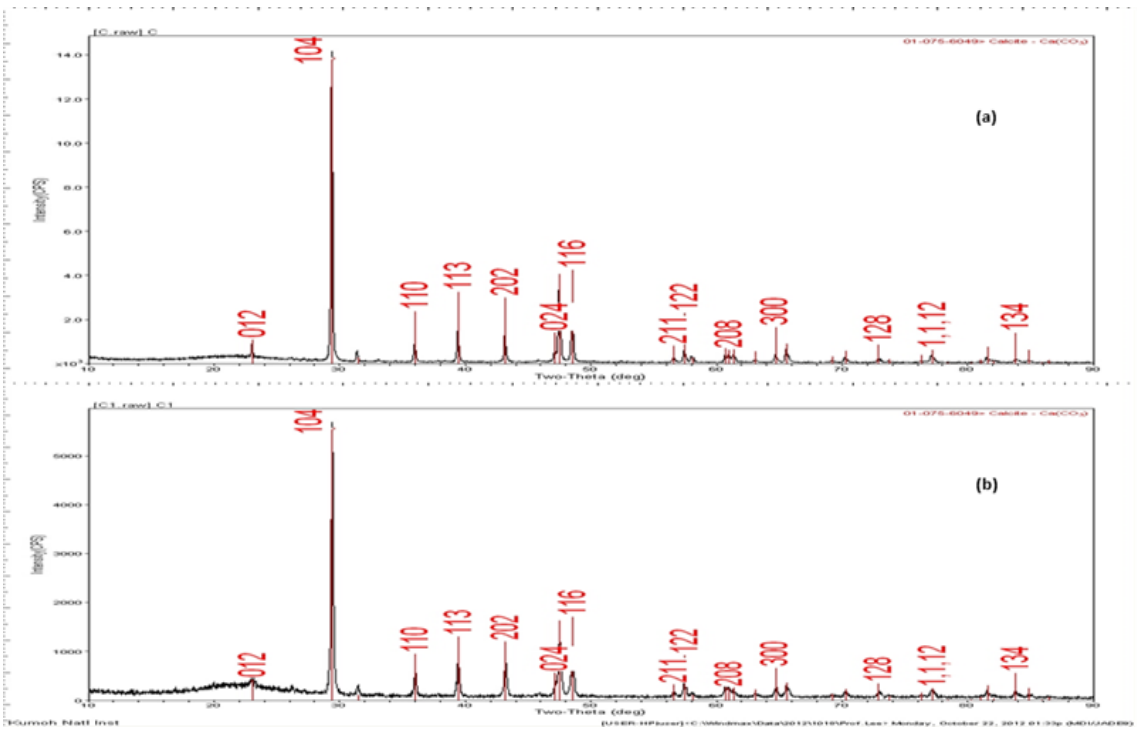

Figure 15: XRPD pattern of powdered oyster shell before SDS adsorption (a) and after SDS adsorption (b).

Wave numbers (cm^{-1})		Corresponding functional groups
Before SDS adsorption	After SDS adsorption	
2881.72	-	Methyne C-H stretching
1640.88	1640.88	Alkenyl C=C stretching
1002.95, 1089.44	1004.23, 1089.02	Aliphatic fluoro compounds (C-F stretching)
625.94, 661.58	626.72, 661.40	Aliphatic bromo compounds (C-Br stretching)
737.34	-	Aliphatic chloro compounds (C-Cl stretching)
1002.95, 1089.44, 1150.05	1004.23, 1089.02, 1162.10	Aromatic C-H in-plane bending
625.94, 661.58, 737.34, 831.26	626.72, 661.40, 830.68	Aromatic C-H out-of-plane bending
3495.82	3470.64	Alcohol, hydroxy group, H-bonded O-H stretching (broad)
1324.44	1324.62	1° or 2°, OH in-plane bending
1406.07, 1324.44	1324.62, 1405.71	Phenol or 3° alcohol, OH bending
625.94, 661.58	626.72, 661.40	Alcohol, OH out-of-plane bending
1089.44	1089.02	Alkyl substituted ether, C-O stretching (C-O-C)
1089.44	1089.02	Cyclic ethers, large rings, C-O stretching
3495.82	3470.64	Aromatic 1° amine (N-H stretching)
1640.88	1640.92	1° amine (N-H bending)
1150.05	1162.10	2° amine (C-N stretching)
1324.44	1324.62	Aromatic 3° amine (C-N stretching)
1324.44, 1406.07	1324.62, 1405.71	Carboxylate (carboxylic acid salt)
1640.88	1640.92	Amide
1707.94	1708.14	Carboxylic acid or ketones
1324.44, 1514.31	1324.62, 1514.23	Aromatic nitro compounds
1002.95	1004.23	Aliphatic phosphates (P-O-C stretching)
1089.44	1089.02	Organic siloxane (silicon-oxy compounds) (Si-O-Si) or (Si-O-C)

Table 2: IR absorption bands and corresponding possible functional groups of lignite and coconut shell-based activated carbon fiber prior to and after SDS adsorption.

(0.41%) > Mg (0.14%). Similarly, the percentage (wt%) of all elements present in powdered oyster shell was investigated as following order (after SDS adsorption): O (50.30%) > Ca (39.95%) > C (8.09%) > Sn (0.80%) > S (0.36%) >Si (0.30%) > Mg (0.20%) (Figure 12).

EDX revealed that, the energy spectra of the x-rays character in powdered pine cones emitted from the elements of C, O, and Cl before and after SDS adsorption indicating no change in elemental composition in the samples after subjected to the surfactant adsorption. Similar condition was observed in case of lignite and coconut shell-based ACF where energy spectra of the x-rays character emitted from the elements of C, O, P, and Na. On the contrary, the energy spectra of the x-rays character in powdered oyster shells emitted from the elements of C, O, Mg, S, Ca, and Sn prior to adsorption, while energy spectra get emitted from the elements of O, Ca, C, Sn, S, Si, and Mg aftermath of surfactant adsorption suggesting the change in elemental composition in the samples after subjected to the surfactant adsorption.

The result from SEM-EDX showed that the concentration and distribution of elements were different prior to and after SDS adsorption in the biosorbents. High percentage of elements (C and O) showed in cluster, while the low percentage of element (Cl) showed wide distribution in powdered cones sample. High percentage of elements (C and O) showed in cluster, while the low percentage of elements (Na and P) showed wide distribution in ACF. Further, SEM-EDX analysis revealed that high percentage of elements (C, O, Ca, and Sn) showed in cluster, while low percentage of the elements (Mg, S) depicted wide distribution in powdered oyster shell before the surfactant adsorption. At the same time, SEM-EDX analysis revealed that high percentage of elements (C, O, Ca, and Sn) showed in cluster, while low percentage of the elements (Mg, S, and Si) depicted wide distribution in powdered oyster shell after the surfactant adsorption [5,6,9].

XRD studies

As seen in Figure 13, partial interference that results the complex pattern as detected by the powder X-ray diffraction suggested amorphous character in the *Pinus densiflora* cone powder. The two broad Bragg or diffraction peaks were observed at around 22° and 34° in both vividly indicated that the adsorption process merely results very little change in surface structure of adsorbent. Similarly, as shown in Figure 14, partial interference that results the complex pattern as detected by the powder X-ray diffraction suggested amorphous character in the lignite and coconut shell-based activated carbon fiber. The two broad Bragg or diffraction peaks were observed at around 20° and 44° in both vividly indicated that the adsorption process merely results very little change in surface structure of adsorbent.

As depicted in the Figure 15, the x-ray powdered diffraction (XRPD) pattern (diffractogram) of all data sets were sharp which indicates that the sample of powdered oyster shell is crystalline material, i.e., crystalline in nature. It was found that oyster shell is entirely composed of $CaCO_3$ and other minerals of trivial amount. The mineral phase of calcium carbonate turns out to be calcite (the mineral $CaCO_3$ of calcite structure is a dominant component of oyster shell).

From the study, it was concluded that the crystal system present in the sample is 'rhombohedral', with Bravais lattice of primitive nature and axial system of a=b=c (axial distance), $\alpha=\beta=\gamma\neq 90°$ (axial angles). The lattice parameter of rhombohedral crystal system is 4.988 × 4.988 × 17.061 Å (90° × 90° × 120°).

Conclusion

The lignite and coconut shell-based ACF and two naturally occurring pine cones, including oyster shells were studied by FE-SEM, XRD, ATR-FTIR spectroscopy, SEM-EDX imaging to determine their chemical, elemental, textural, and structural properties. In

Wavenumbers (cm^{-1})		Corresponding functional groups
Before SDS adsorption	After SDS adsorption	
2883.08	2878.84	Methyne C-H stretching
1629.71	1629.03	Alkenyl C=C stretching
1089.65	1089.48	Aliphatic fluoro compounds (C-F stretching)
625.47	625.77	Aliphatic bromo compounds (C-Br stretching)
711.60	711.59	Aliphatic chloro compounds (C-Cl stretching)
1089.65, 1150.78	1089.48, 1139.74	Aromatic C-H in-plane bending
625.47, 711.60, 876.94	625.77, 711.59, 875.60	Aromatic C-H out-of-plane bending
3483.47	3483.23	Alcohol, hydroxy group, H-bonded O-H stretching (broad)
1327.59	1327.04	1° or 2° alcohol, OH in-plane bending
1327.59	1327.04	Phenol or 3° alcohol, OH bending
625.47, 711.60	625.77, 711.59	Alcohol, OH out-of-plane bending
1089.65	1089.48	Alkyl substituted ether, C-O stretching (C-O-C)
3483.47	3483.23	Heterocyclic amine, N-H stretching
3483.47	3483.23	Aromatic 1° amine (N-H stretching)
1629.71	1629.03	1° amine (N-H bending)
1150.78	1139.74	2° or 3° amine (C-N stretching)
1282.30, 1327.59	1283.10, 1327.04	Aromatic 1° or 2° or 3° amine (C-N stretching)
1629.71	1629.03	2° amine, N-H bending
1327.59, 1413.59	1327.04, 1414.47	Carboxylate (carboxylic acid salt)
1707.24	1706.83	Carboxylic acid or ketones
1798.11	1797.73	Acid (acyl) halide (Haloformyl) (RCOX) (X = F, Cl, I, Br)
1089.65, 1150.78	1089.48, 1139.74	Cyanate (-OCN and C-OCN stretching)
1327.59	1327.04	Aromatic nitro compounds
1282.3, 1327.59	1283.10, 1327.04	Organic phosphates (P=O stretching)

Table 3: IR absorption bands and corresponding possible functional groups of powdered oyster shell prior to and after SDS adsorption.

addition, the samples were treated to determine the iodine number. The XRD analysis suggested the amorphous character in lignite and coconut shell-based ACF and powdered *Pinus densiflora* cones, while it indicated that the sample of powdered oyster shell is crystalline in nature and entirely composed of $CaCO_3$ with the very trivial amount of impurities. In addition, XRPD pattern indicated that the adsorption process merely results very little change in surface structure of aforementioned biosorbents.

The SEM-EDX analysis indicated that the concentration and distribution of elements were different prior to and after SDS adsorption in the biosorbents. Similarly, the FE-SEM imaging at three different magnifications depicted the change in surface texture and morphology in all three biosorbent samples prior to and aftermath of surfactant adsorption. The IR spectroscopy demonstrated the variation in IR spectra of the samples prior to and after surfactant adsorption and also further suggested occurrence of complexing or (complexation) process between ionizable functional groups present on the surface of biosorbent samples and DS^{-}or Na^{+} ions of SDS. The chemical, elemental, and micro-structural aspects of the aforementioned samples are likely to play an important role in adsorption process.

Acknowledgements

The present study was financially supported by Korea Research Foundation Grant funded by the Korean Government.

References

1. Chowdhury ZZ, Zain SM, Rashid AK, Ahmed AA, Khalid K, et al. (2012) Application of response surface methodology (RSM) for optimizing production condition for removal of Pb (II) and Cu (II) onto Kenaf Fiber Based Activated Carbon. J Appl Sci Eng Technol 4: 458-465.
2. Özacar M, Sengil ÌA, Türkmenler H (2008) Equilibrium and kinetic data, and adsorption mechanism for adsorption of lead onto valonia tennin resin. Chem Eng J 143: 32-42.
3. Chowdhury ZZ, Zain SM, Rashid AK, Rafique RF, Khalid K (2012) Breakthrough curve analysis for column dynamics sorption of Mn (II) ions from wastewater by using Mangostana garcinia peel-based granular activated carbon. J Chem.
4. Persson P, Axe K (2005) Adsorption of oxalate and malonate at the water-goethite interface: molecular surface speciation from IR spectroscopy. Geochim Cosmochim Acta 69: 541-552.
5. Coates J (2000) Interpretation of infrared spectra, a practical approach. Encyclopedia of Analytical Chemistry. Meyers RA (ed), John Wiley & Sons Ltd, Chichester, p: 10815-10837.
6. Velasquez P, Leinen D, Pascual J, Ramos-Barrado JR, Cordova R, et al. (2001) XPS, SEM, EDX and EIS study of an electrochemically modifed electrode surface of natural chalcocite (Cu_2S). J Electroanal Chem 510: 20-28.
7. Charalambous FA, Ram R, Pownceby MI, Tardio J, Bhargava SK (2012) Chemical and microstructural characterization studies on natural and heat treated brannerite samples. Miner Eng 39: 275-288.
8. Yoon GL, Kim BT, Kim BO, Han SH (2003) Chemical-mechanical characteristics of crushed oyster-shell. Waste Manag 23: 825-834.
9. Qiu Y, Zhang Q, Tian Y, Zhang J, Cao J, et al. (2011) Composition and structure of luxing coal with different particles sizes. Pet Coal 53: 45-55.